LINEAR CHARGED-PARTICLE ACCELERATORS

AN ACCELERATING CHANNEL OF INTERMEDIATE PART OF HIGH-CURRENT PROTON LINAC BASED ON COMBINED FOCUSING BY RF FIELD

S.S. Tishkin, M.G. Shulika, O.M. Shulika
National Science Center "Kharkov Institute of Physics and Technology", Kharkiv, Ukraine
E-mail: tishkin@kipt.kharkov.ua

Particle dynamics in an accelerating-and-focusing channel of intermediate part of a proton linac based on combined rf-focusing under following conditions: energy range 3…100 MeV, current 100 mA, and acceleration rate 5 MeV/m, is studied. To implement combined rf-focusing, it is proposed to use accelerating structures of two different types: an Interdigital IH-type structure allows acceleration in the range of 3 to 20 MeV, while a Crossbar CH-type structure accelerates particles from 20 up to 100 MeV. Also, methods to adjust rf-field amplitude in quadrupole gaps for both (IH and CH) structures are discussed.

PACS: 29.+w

INTRODUCTION

Investigations focused on safety of nuclear power engineering are associated with ion accelerators operating at high energy (up to 1 GeV) and current in the range of 20…30 mA [1, 2]. To provide the safe radiation background, it is very important to decrease particle losses through an accelerating channel. It could be done by choosing the appropriate methods for particle motion stability at different energy ranges. In general, an accelerator is comprised of the following parts: an injector (the energy range of 70…100 keV), an initial accelerator part yielding the output energy about 2…3 MeV, an intermediate section where particles are accelerated to about 100…150 MeV, and a main part for the energies of 1.0…1.7 GeV. The intermediate section that usually consists of a series of drift tubes along with electromagnetic (or solid) lenses as focusing elements is that particular part that contributes the most to the radiation background.

In this paper, an accelerating and focusing channel of medium energy range based on combined rf-focusing (CRFF) featuring the high acceleration rate and small beam losses is considered [3, 4].

ACCELERATING AND FOCUSING CHANNEL MODIFICATIONS, THEIR PARAMETERS AND IMPLEMENTATION

If the charged particles are focused by the electric rf-field itself then the whole accelerating structure could be simplified in design. Fig. 1 depicts the accelerating and focusing period of a high-current proton linac based on CRFF for the energy range of 3…40 MeV. The upper energy value (40 MeV) is the maximum possible for proton acceleration in the IH-structure.

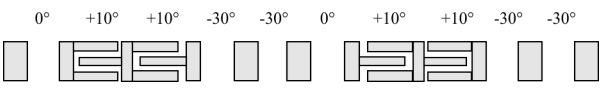

Fig. 1. Structure of the accelerating and focusing period and synchronous phase distribution in accelerating gaps (type I)

The main characteristics of the linac are the following: the energy range is 3…40 MeV, the operating frequency is 350 MHz, the channel of 740 cm in length is divided into 94 accelerating gaps, the aperture radius varies from 0.75 to 1.0 cm.

Table 1

Input and output beam emittances

Input beam parameters			
I, mA	ε_x(rms), mm·mrad	ε_y(rms), mm·mrad	ε_z(rms), keV·degrees
0	0.243	0.241	192.73
100			
Output beam parameters			
I, mA	ε_x(rms), mm·mrad	ε_y(rms), mm·mrad	ε_z(rms), keV·degrees
0	0.253	0.250	238.94
100	0.287	0.309	245.20

Table 2

Input Twiss parameters, transverse emittance growth and beam transmission coefficient

Input beam parameters				
I, mA	α_x	β_x, cm/rad	α_x	β_x, cm/rad
0	-0.0107	55.27	0.0072	11.42
100	-0.0106	98.26	0.0074	20.30
Output beam parameters				
I, mA	$\Delta\varepsilon_x$, %	$\Delta\varepsilon_y$, %	T_p, %	
0	4.1	3.7	100	
100	18.1	28.2	100	

Table 1 gives input and output normalized emittances obtained at two different injection current values. Table 2 lists Twiss parameters α_x, β_x, α_y, β_y of the beam consistent with the channel, growth of the transverse beam emittances $\Delta\varepsilon_x$, $\Delta\varepsilon_y$, and the beam transmission coefficient T_p. The choice for the input current value is based on the following consideration: beam dynamics calculation at zero injection current provides the emittance growth only due to the rf-field with Coulomb forces not being taken into account. As it follows from Table 2, at zero injection current the emittance growth is rather small ($\Delta\varepsilon_x$ = 4.1%, $\Delta\varepsilon_y$ = 3.7%), so, the influence of the rf-field on the emittance growth is negligible for CRFF. Pulse current of 100 mA is the

rated current for this linac. The emittance growth of $\Delta\varepsilon_x$ = 18.1%, $\Delta\varepsilon_y$ = 28.2% at T_p=100% are also reasonable.

As the IH-structure can provide proton acceleration only up to 30…40 MeV, to accelerate the protons to higher energy (from 30…40 to 100 MeV) the CH-structure must be used. The CH-structure provides acceleration up to 150 MeV at the frequency of 700 MHz. Fig. 2 illustrates the half of the focusing period in the CH-structure, while Fig. 3 presents the possible general view of the CRFF-based CH-structure as the intermediate part of the high-current proton linac.

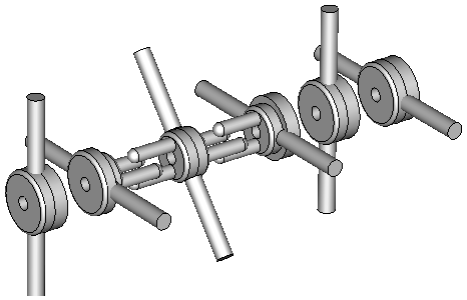

Fig. 2. Half of the focusing CRFF-based period, the CH-structure

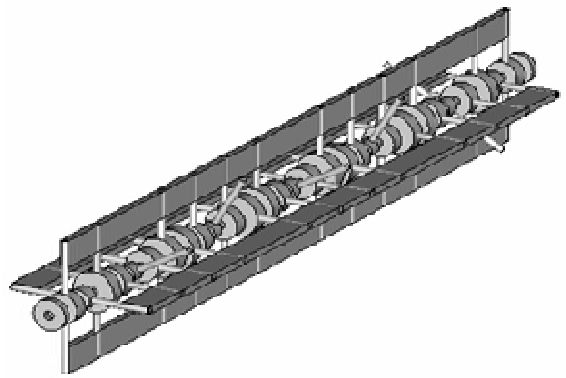

Fig. 3. General view of the CH-structure for the linac intermediate part (cavity walls are not shown)

The quadrupole field component is generated by the additional electrodes inserted into the accelerating gap. As the introduction of these additional electrodes reduces the electrical strength of the quadrupole segment, it is necessary to decrease the potential difference across the quadrupole segment in reference to the voltage drop across the axisymmetric gaps. Moreover, the higher the particle velocity, the larger the difference between the voltage drop across the quadrupole and the axisymmetric segments. This is due to the fact that for effective acceleration the potential difference across the axisymmetric gap is proportional to the relative velocity β, while the voltage difference is limited across the quadrupole segment by its electrical strength and remains almost constant along the accelerating structure. This leads to necessity of 'smooth' increase in potential difference between the quadrupole segment and the axisymmetric gap along the accelerating and focusing channel.

In case of the IH-structure, the tuning is achieved by the azimuthal rotation of the shaft holding the central drift tube of the quadrupole segment. As for the CH-structure, two shafts of the quadrupole segment are rotated to accomplish the tuning (see Figs. 2 and 3). This tuning technique allows one to vary the potential difference across the quadrupole segment from zero (the angle between the quadrupole segment shaft and any neighboring one equals 0°) to the maximum which is equal to the voltage drop across the axisymmetric gap (the angle is 180° for the IH-structure and 90° for the CH-structure). Thus, by changing the angle the necessary voltage difference between any neighboring quadrupole and axisymmetrical gap can be obtained [3].

It is worth to notice, the concept of combined rf-focusing is limited by neither energy range nor the type of particle being accelerated. Here, we are dealing with the structure efficiency. It is obvious that the implementation of CRFF on the basis of the CH-structure discussed above is not unique. CRFF can be put to use in the accelerator consisting of one-, two- or three-gap cavities. If this is the case, an external focusing element can be substituted by a combination of the rf quadrupole cavities and the axisymmetrical gaps.

The simulation of beam dynamics in the CRFF-based channel for output energy of 40 MeV demonstrates that the 100 mA beam is accelerated almost with no particle losses at the acceleration rate of 5 MeV/m showing low emittance growth ($\Delta\varepsilon_x$=18.1%, $\Delta\varepsilon_y$=28.2%).

Another modification of the accelerating and focusing channel based on CRFF is presented in Fig. 4. This modification differs from the previous one (see Fig. 1) in the distribution of synchronous phases. Here the synchronous phase is identical over all the gaps and equals -20°. This makes the structure more uniform and easier to adjust the rf-field amplitude as there is no phase transit -30° → 0°. Next, the synchronous phase over the quadrupole gap is changed from +10° to 0°. As has been shown in Ref. [3], the small positive synchronous phase over the quadrupole gap expands the domain of transverse particle stability if phase fluctuations are disregarded. However, in practice, the phase oscillations enlarge 'automatically' the domain of radial particle stability and smooth the phase shift of radial oscillation for asynchronous particles. As the focusing rigidity of the rf quadrupole is proportional to $\cos\varphi$ (φ being the transit phase), then the replacement +10° → 0° reduces the electric field intensity over the quadrupole segment.

The numerical simulation of beam dynamics in both channels shows no significant differences in the emittance growth during acceleration process. In practice terms, the accelerating and focusing channel of type II (see Fig. 4) is preferable to the channel of type I (see Fig. 1).

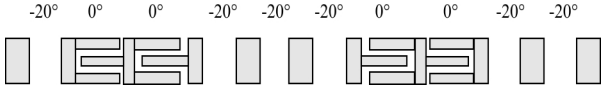

Fig. 4. Structure of the accelerating and focusing period and synchronous phase distribution in accelerating gaps (type II)

To simulate the accelerating and focusing channel of the accelerator intermediate part with combined rf focusing and beam dynamics within it, the APFRFQ code was used [3]. Following are the main parameters: the energy range is 3…100 MeV, the operating frequency is 350 MHz, the channel of 18.44 m in length is divided

into 160 accelerating gaps, the aperture radius varies from 0.8 to 1.1 cm. The channel is divided into 16 focusing segments. Each focusing segment consists of 10 accelerating gaps, 6 of which are axisymmetrical and 4 – RFQ. The focusing segment has a FOOODDOOOF pattern (with F being the focusing gap in a transverse plane, O representing the axisymmetrical gap, and D standing for the defocusing area). The synchronous particle phase over the axisymmetrical and quadrupole gap is -20° and 0°, respectively. The electric field strength is calculated by a method of auxiliary charges. The electric field maximum of 200 kV/cm is on the axisymmetrical gap axis. The average field gradient over the quadrupole gap is 160 kV/cm^2. While simulating beam dynamics, the focusing field across the quadrupole gap is set to be linear. The aperture radius of the channel is determined by the field gradient providing the necessary electrical strength of the gap. The electric field intensity maximum on the electrode surface is adopted as the criterion of electrical strength. In calculations, it is assumed to be of 366 kV/cm or $2K_p$ (K_p is Kilpatrick criterion).

To account for the space-charge effects, a macroparticle (particle – particle) method involving 3600 simulation particles was used. Fig. 5 presents the main input and output parameters, i.e. the transverse emittances, the beam phase portrait, and the beam geometric projection on the XY plane calculated at zero injection current. The same parameters calculated at 100 mA injection current are depicted in Fig. 6. Table 3 lists the main calculated quantities for the accelerated beam at zero and 100 mA injection current.

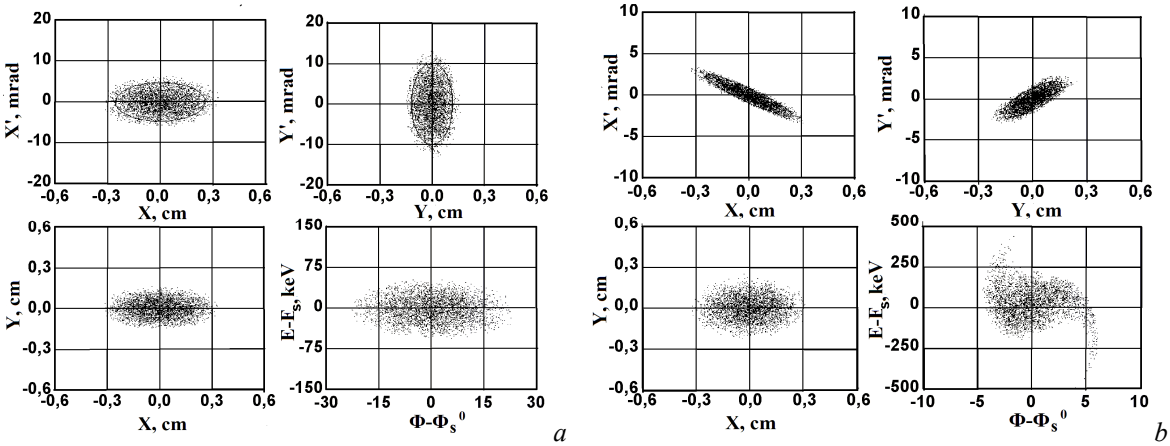

Fig. 5. Beam characteristics, output energy 100 MeV at zero injection current: input (a); output (b)

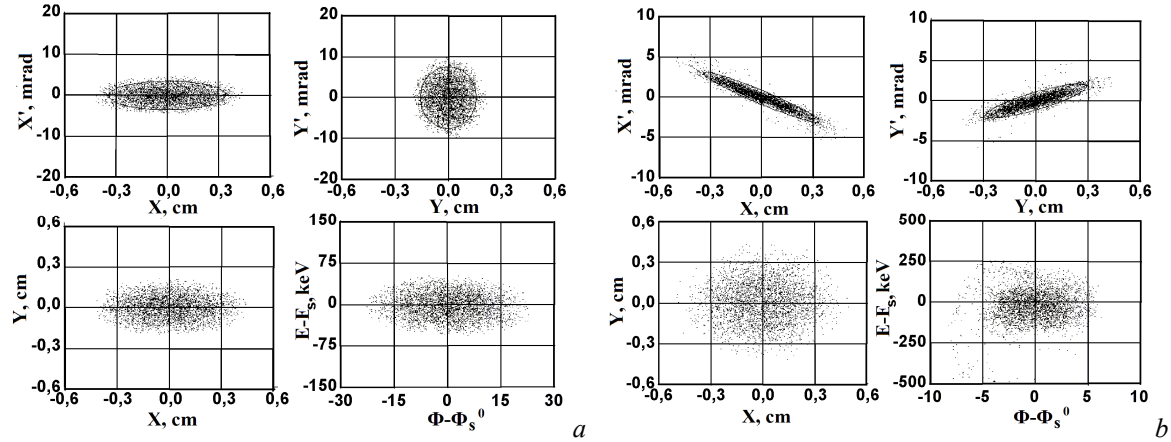

Fig. 6. Beam characteristics, output energy 100 MeV at 100 mA injection current: input (a); output (b)

One of the conditions for retardation of emittance growth lies in independency of focusing forces from the transit phase over the focusing period. In general, this condition is not met in an accelerator with conventional rf-focusing – focusing forces do depend on transit phase. During acceleration process, nonlinear fluctuations of asynchronous particles occur about the synchronous particle phase. The coupling between the longitudinal and transverse motion can give rise to the emittance growth even under linear focusing field and/or in the absence of Coulomb forces. An accelerator based on the alternating-phase focusing exhibits such properties especially at low energy.

Table 3

Summary of beam emittances calculated

Quantaties	Input	Output	
		(I=0 mA)	(I=100 mA)
ε_x(rms), mm·mrad	0.242	0.256	0.357
ε_y(rms), mm·mrad	0.236	0.256	0.379
ε_z(rms), keV·degrees	188.5	239.5	253.6
ε_x(99%), mm·mrad	1.485	1.630	5.226
ε_y(99%), mm·mrad	1.466	1.768	4.202
ε_z(99%), keV·degrees	1191.1	2823.6	4192.4

The computer simulation of particle dynamics at zero injection current establishes the influence of rf field on the transverse emittance growth in the absence of Coulomb forces. In this case, the increase in emittance is small and about 5%. In the case of 100 mA injection current, the beam emittance growths up to 60% that still is acceptable. The beam transmission coefficient is 100%.

CONCLUSIONS

The absence of the external focusing devices together with simplicity in design makes CRFF effective for superconducting cavity structures as well. In this case, a superconducting structure already designed, studied and manufactured can be transformed into a CRFF-based one by the certain upgrade. By way of example, the accelerating channel operating at the energy range of 20…100 MeV can be assembled using 2- and 3-gap superconducting spoke cavities. To do this, the additional 'horned' electrodes generating quadrupole field component are to be inserted into the accelerating gap of 2-gap cavity. With the independent power supply this assembly forms the RFQ-unit with adjustable strong focusing. Acceleration along with beam phase stability occurs in the 3 (or 5)-gap cavity.

REFERENCES

1. C. Rubbia. Status of the Enegy Amplifar Concept // *Proc. II Int. Conf. ADTT and A*, Kalmar, Sweden. 1996, p. 35.
2. N.A. Khizhnyak. Safe Electronuclear Power Industry // *Proc. II Int. Conf. ADTT and A*, Kalmar, Sweden. 1996, p. 395.
3. S.S. Tishkin. Combined focusing by RF-field for ion linac accelerators // *Journal of Kharkiv National University. Physical Series "Nuclear, Particle, Fields"*. 2008, № 808, Issue 2(38), p. 37-46.
4. S.S. Tishkin, M.G. Shulika, O.M. Shulika. Ion beam propagation stability in a linac accelerating channel with combined rf focusing // *Problems of Atomic Science and Technology. Series "Nuclear Physics Investigations"*. 2019, № 6, p. 94-99.

Article received 24.02.2020

УСКОРЯЮЩИЙ КАНАЛ ПРОМЕЖУТОЧНОЙ ЧАСТИ СИЛЬНОТОЧНОГО ЛИНЕЙНОГО УСКОРИТЕЛЯ ПРОТОНОВ С КОМБИНИРОВАННОЙ ФОКУСИРОВКОЙ ВЫСОКОЧАСТОТНЫМ ПОЛЕМ

С.С. Тишкин, Н.Г. Шулика, О.Н. Шулика

Исследована динамика частиц в ускоряюще-фокусирующем канале промежуточной части протонного ускорителя с комбинированной высокочастотной фокусировкой в диапазоне энергий 3…100 МэВ для 100 мА тока с темпом ускорения 5 МэВ/м. Предложена схема реализации данного варианта фокусировки на базе двух типов ускоряющих структур. В диапазоне энергий 3…20 МэВ предложено использовать IH-структуру, а в диапазоне 20…100 МэВ – CH-структуру. Рассмотрены методы настройки амплитуды высокочастотных полей в квадрупольных зазорах для IH- и CH-структур.

ПРИСКОРЮЮЧИЙ КАНАЛ ПРОМІЖНОЇ ЧАСТИНИ СИЛЬНОСТРУМОВОГО ЛІНІЙНОГО ПРИСКОРЮВАЧА ПРОТОНІВ З КОМБІНОВАНИМ ФОКУСУВАННЯМ ЗА ДОПОМОГОЮ ВИСОКОЧАСТОТНОГО ПОЛЯ

С.С. Тішкін, М.Г. Шуліка, О.М. Шуліка

Досліджено динаміку частинок у каналі, що прискорює та фокусує, середньої частини протонного прискорювача з комбінованим високочастотним фокусуванням у діапазоні енергій 3…100 МеВ для струму 100 мА з темпом прискорення 5 МеВ/м. Запропоновано схему реалізації даного варіанту фокусування на основі двох типів структур, що прискорюють. У діапазоні енергій 3…20 МеВ запропоновано використовувати IH-структуру, а для діапазону енергій 20…100 МеВ – CH-структуру. Розглянуто методи налаштування амплітуди високочастотних полів у квадрупольних зазорах для IH- та CH-структур.